Aquatic Sciences (2026) 88:29
https://doi.org/10.1007/s00027-025-01263-2

Aquatic Sciences

RESEARCH ARTICLE

Methanogenesis pathways and methane oxidation in two clear-water and two turbid-water urban ponds in Brussels (Belgium)

Alberto V. Borges[1] · **Nathalie Gypens**[2] · **Thomas Bauduin**[1,2]

Received: 25 May 2025 / Accepted: 29 December 2025

Abstract

Ponds are a large source of atmospheric methane (CH_4), a potent greenhouse gas, resulting from the net balance between input from sedimentary methanogenesis and removal by CH_4 oxidation (MOX). Here, we test whether methanogenesis pathways (acetoclastic or hydrogenotrophic) and MOX might differ between clear-water (macrophyte-dominated) and turbid-water (phytoplankton-dominated) ponds. We measured the $^{13}C/^{12}C$ ratio of CH_4 ($\delta^{13}C$-CH_4) from gas trapped in bubble traps, from bubbles deliberately released by the perturbing sediments, and in dissolved CH_4 in the water column in four urban ponds in Brussels, Belgium (Leybeek, Pêcheries, Tenreuken, Silex). In summer, the $\delta^{13}C$-CH_4 values of sediment bubbles indicated that the hydrogenotrophic methanogenesis pathway appeared to be more important in clear-water (macrophyte-dominated) ponds (Leybeek and Pêcheries), whereas the acetoclastic methanogenesis pathway appeared to be more important in turbid-water (phytoplankton-dominated) ponds (Tenreuken and Silex). The $\delta^{13}C$-CH_4 values from bubble traps indicated a seasonal shift from acetoclastic methanogenesis pathway in spring–summer to hydrogenotrophic methanogenesis in fall. The $\delta^{13}C$-CH_4 of dissolved CH_4 indicated higher rates of MOX in turbid-water ponds (Leybeek and Pêcheries) compared to clear-water ponds (Tenreuken and Silex), with an overall positive relation with total suspended matter and chlorophyll-a concentrations. The presence of suspended particles likely enhanced MOX by reducing light inhibition of MOX and/or by serving as substrates in the water column for attached methanotrophic bacteria. MOX represented ~ 80% of the total dissolved CH_4 removal from the water column (MOX plus diffusive emission to the atmosphere) in the turbid-water ponds (Leybeek and Pêcheries) and < 60% in the clear-water ponds (Tenreuken and Silex). Our results suggest that shifts from clear- to turbid-water ecological states due to eutrophication may change CH_4 production pathways (with a higher contribution of acetoclastic versus hydrogenotrophic methanogenesis) and enhance dissolved CH_4 removal by MOX in the water column.

Keywords Urban ponds · Methane emissions · Methane oxidation · Hydrogenotrophic methanogenesis · Acetoclastic methanogenesis · Methane carbon stable isotopes

Introduction

Inland waters (rivers, lakes, and reservoirs) are quantitatively important sources of greenhouse gases to the atmosphere (Lauerwald et al. 2023). Lakes and ponds are particularly strong sources of methane (CH_4) and represent the second-largest aquatic CH_4 source after freshwater wetlands (Rosentreter et al. 2021). The CH_4 emissions from lakes and ponds reflect the net balance between CH_4 inputs from methanogenesis in sediments, soils, and groundwater, and removal by microbial CH_4 oxidation (MOX) in sediments and the water column. Between 60 and 90% of CH_4 produced in lake sediments is consumed by MOX, efficiently mitigating CH_4 emissions (Rudd and Hamilton 1978; Bastviken et al. 2002, 2008; Kankaala et al. 2006, 2007; Durisch-Kaiser et al. 2011; Morana et al. 2015; Singleton et al. 2018; Thottathil et al. 2018, 2019; Mayr et al. 2020).

MOX occurs aerobically, using oxygen (O_2) as the electron acceptor, and anaerobically, using alternative electron acceptors such as sulphate (SO_4^{2-}), nitrate (NO_3^-), manganese/iron (Mn/Fe) oxides. In fresh waters, because these alternative electron acceptors are relatively scarce, most CH_4 removal by MOX occurs under aerobic conditions (Rudd

---

✉ Alberto V. Borges
alberto.borges@uliege.be

[1] Chemical Oceanography Unit, University of Liège, Liège, Belgium

[2] Ecology of Aquatic Systems, Université Libre de Bruxelles, Brussels, Belgium

et al. 1974; Lopes et al. 2011; Roland et al. 2018; Sturm et al. 2019). The CH_4 and O_2 availability are the major factors regulating the abundance and activity of aerobic CH_4-oxidizing bacteria and therefore MOX rates (Rudd and Hamilton 1978; Utsumi et al. 1998; Shelley et al. 2014; Thottathil et al. 2018, 2019; Reis et al. 2020, 2022). Methanotrophs respond rapidly to favourable CH_4 and O_2 conditions following environmental changes (e.g. vertical mixing) (Mayr et al. 2020; Reis et al. 2020). MOX is inhibited by NH_4^+ addition (Bosse et al. 1993; Murase and Sugimoto 2005) and by light (Dumestre et al. 1998; Murase and Sugimoto 2005; Morana et al. 2020). In the water column, MOX increases with temperature (Thottathil et al. 2019; Iwata et al. 2020), while MOX in lake sediments appears relatively insensitive to temperature changes, according to Duc et al. (2010). MOX has been shown to increase in rivers with total suspended matter (TSM) content, due to a higher abundance of particle-attached methanotrophs (Abril et al. 2007).

Methanogenesis proceeds via three main metabolic pathways (Borrel et al. 2011). Hydrogenotrophic methanogenesis reduces carbon dioxide (CO_2) to CH_4 using H_2 generated by microbial fermentation; methanogens and fermenters form syntrophic consortia because methanogenesis maintains low H_2 concentrations necessary for fermentation. Acetoclastic methanogenesis cleaves acetate, oxidizing the carboxyl group to CO_2 and reducing the methyl group to CH_4. Methylotrophic methanogenesis produces CH_4 by reducing methyl groups from methylated compounds (e.g. methanol, trimethylamines, methyl sulphides). Methylotrophic methanogenesis is expected to be minor in freshwater lakes because methylated compounds are relatively scarce; thus, methanogenesis is expected to proceed mainly via hydrogenotrophic and acetoclastic pathways. Based on theoretical H_2-to-acetate ratios from fermentation, hydrogenotrophic methanogenesis is predicted to account for ~ 30% of overall methanogenesis in freshwater lakes (Conrad 1999). Methanogenesis rates in lake sediments are positively linked to trophic status (Duc et al. 2010; Grasset et al. 2018) and temperature (Zeikus and Winfrey 1976). Availability of alternative electron acceptors (SO_4^{2-}, NO_3^-, Mn/Fe oxides) indirectly affects methanogenesis rates because SO_4^{2-}-, iron-reducing, and denitrifying bacteria outcompete methanogens for H_2 and acetate (Winfrey and Zeikus 1979; Achtnich et al. 1995).

To date, there is no direct evidence for methylotrophic methanogenesis in lake sediments (Su et al. 2025). Methylotrophic methanogenesis has been shown to be important only in SO_4^{2-}-reduction zones of marine sediments (Xu et al. 2021). Acetoclastic methanogenesis was traditionally assumed to dominate in lake sediments (Whiticar 1999; Whiticar et al. 1986), but more recent evidence shows hydrogenotrophic methanogenesis can be dominant (Conrad et al. 2011; Meier et al. 2024; Su et al. 2025). In Lake Geneva sediments, there was no clear influence of organic carbon source (phytoplankton versus terrestrial) on the dominant methanogenic pathway (Su et al. 2025).

CH_4 produced by acetoclastic and hydrogenotrophic pathways exhibits distinct $^{13}C/^{12}C$ ratios ($\delta^{13}C$–CH_4) (− 65‰ to − 50‰ versus − 100‰ to − 60‰, respectively) (Whiticar et al. 1986), which can be used to infer the dominant pathway. Methanotrophs preferentially consume $^{12}CH_4$, resulting in an enrichment in ^{13}C of the residual CH_4 in the water column, which can be used to estimate MOX with isotopic fractionation models (Bastviken et al. 2002).

Shallow ponds occur in two alternative ecological states determined by dominant primary producers: a clear-water state dominated by submerged macrophytes and a turbid-water state dominated by phytoplankton (Scheffer et al. 1993). Eutrophication drives the shift from clear- to turbid-water states, altering food webs (Jeppesen et al. 1999), although the shift is complex and context dependent (Scheffer and van Nes 2007; Davidson et al. 2023). It remains unclear how these two states affect CH_4 dynamics and emissions from ponds.

Bauduin et al. (2025) recently quantified seasonal variations of CH_4 concentrations and emissions in four urban ponds in the city of Brussels. The Leybeek and Pêcheries ponds are turbid-water systems [higher chlorophyll-a (Chl-a) and TSM concentrations, and lower macrophyte cover] while the Tenreuken and Silex ponds are clear-water systems (Table 1). Bauduin et al. (2025) found no significant differences among the four ponds in dissolved CH_4 concentrations and diffusive CH_4 emissions ($F_{diff}CH_4$), but ebullitive CH_4 emissions were significantly higher in the two macrophyte-dominated clear-water ponds (Tenreuken and Silex) than in the two phytoplankton-dominated turbid-water ponds (Pêcheries and Leybeek) (Table 1). The dominant submerged macrophyte was the non-rooted species *Lemna trisulca*, which may account for the higher ebullitive CH_4 fluxes observed in the clear-water ponds (Cabrera-Lamanna et al. 2025) (Table 1).

Here, we test the hypothesis that MOX is higher in turbid-water ponds (Pêcheries and Leybeek) than in clear-water ponds (Tenreuken and Silex), due to a higher abundance of particle-attached methanotrophs (Abril et al. 2007) and/or the alleviation of light inhibition of MOX (Morana et al. 2020). We also test whether the methanogenesis pathway (acetoclastic versus hydrogenotrophic) differs between turbid- and clear-water ponds because of differences in sediment organic matter composition and lability. In lentic systems, autochthonous organic matter (phytoplankton and aquatic macrophyte) is more labile and susceptible to methanogenic degradation than allochthonous terrestrial organic matter (Grasset et al. 2018). Whether this affects methanogenesis rates and pathways (Su et al. 2025), and whether differences exist between phytoplankton- and

Table 1 Surface area, average water column depth, macrophyte cover in the summer, mean ± SD of chlorophyll-a (*Chl-a*) and total suspended matter (*TSM*) concentrations during the summer and all seasons, dissolved CH_4 concentration, diffusive CH_4 fluxes (F_{diff}), and ebullitive CH_4 fluxes (F_{ebull}) in four urban ponds in the city of Brussels (Leybeek, Pêcheries, Tenreuken, and Silex) sampled 38 times each from January 2022 to December 2023

	Leybeek	Pêcheries	Tenreuken	Silex
Surface area (ha)	0.7	1.4	3.2	1.0
Average depth (m)	0.6	1.3	1.4	1.1
Macrophyte cover (%) summer	6	9	68	100
Chl-a (μg L^{-1}) all seasons	55.8 ± 44.2	13.2 ± 12.0	8.2 ± 11.3	2.7 ± 4.4
Chl-a (μg L^{-1}) summer	88.8 ± 55.2	21.5 ± 15.7	2.9 ± 2.2	0.9 ± 1.4
TSM (mg L^{-1}) all seasons	39.0 ± 31.8	12.6 ± 9.3	10.5 ± 8.3	6.4 ± 4.7
TSM (mg L^{-1}) summer	56.5 ± 37.4	16.0 ± 11.3	5.9 ± 3.3	5.1 ± 3.3
CH_4 (nmol L^{-1})	3885 ± 8039	2255 ± 2069	2827 ± 6419	4252 ± 3055
F_{diff} CH_4 (mmol m^{-2} day^{-1})	1.7 ± 3.1	1.1 ± 1.1	1.4 ± 3.2	2.1 ± 1.6
F_{ebull} CH_4 (mmol m^{-2} day^{-1})	4.0 ± 5.2	2.5 ± 1.9	7.2 ± 6.9	13.3 ± 10.8

For a detailed description of measurement methods, seasonal variations, statistical tests of difference of means, and putative drivers, refer to Bauduin et al. (2025)

macrophyte-dominated systems (Wang et al. 2023), is unclear and understudied. We also test whether the methanogenesis pathway might change seasonally. We use $\delta^{13}C–CH_4$ measurements of sediment bubbles to infer the relative importance of methanogenic pathways (acetoclastic versus hydrogenotrophic) and $\delta^{13}C–CH_4$ in surface water samples to quantify MOX in four urban ponds in Brussels (Silex, Tenreuken, Leybeek, and Pêcheries) (Fig. 1 and Table 1).

Materials and methods

Site description

Belgium has a temperate climate with mild temperatures and relatively high precipitation. From 1991 to 2020, precipitation and temperature averaged 837 mm and 11 °C, respectively. Summer and winter temperatures averaged 17.9 °C and 4.1 °C, respectively. The ponds in Brussels are artificial, small, shallow, and eutrophic (De Backer et al. 2010; Van Onsem et al. 2010; Peretyatko et al. 2012). Ponds near the city centre lie in recreational parks, while peripheral ponds are within the Sonian Forest. Several ponds are in Natura 2000 protected areas and serve biodiversity and recreational functions (e.g. boating, fishing). According to the classification by Scheffer et al. (1993), Brussels' eutrophic ponds exhibit two alternative stable states: a clear-water state dominated by a few submerged macrophyte species with variable abundance (Peretyatko et al. 2007), and a turbid-water state dominated by phytoplankton—primarily cyanobacteria—which can produce harmful algal blooms (De Backer et al. 2010; Van Onsem et al. 2010; Peretyatko et al. 2012).

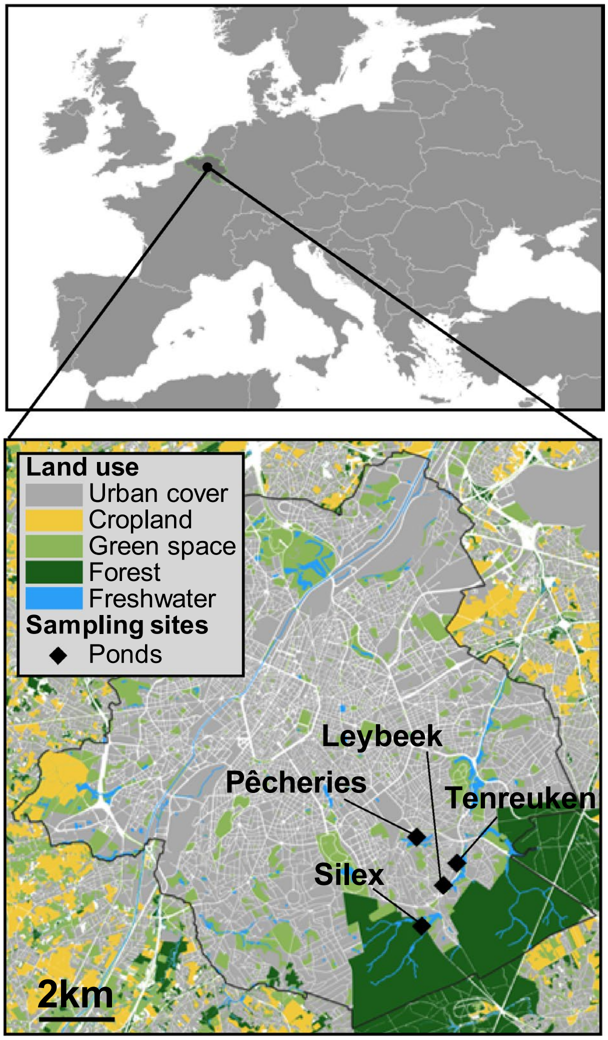

Fig. 1 Location of the four sampled urban ponds (*black diamonds*) in the city of Brussels (Belgium) and land use

This study focuses on four ponds—Leybeek, Pêcheries, Tenreuken, Silex (Fig. 1; Table 1). All of these ponds are relatively small (0.7–3.2 ha) and shallow (0.6–1.4 m) (Table 1), differing mainly in dominant primary producers during spring–summer. Leybeek and Pêcheries are turbid-water ponds with elevated summer Chl-a and TSM, indicative of phytoplankton (mostly cyanobacteria) dominance. Tenreuken and Silex are clear-water ponds with lower Chl-a and TSM and submerged-macrophyte dominance, primarily *Lemna trisulca*. Seasonal and interannual variations in dissolved CO_2, CH_4, and N_2O concentrations and emissions in these ponds have been documented in companion studies (Bauduin et al. 2024, 2025), but their methanogenesis pathways and MOX are unknown.

Sample collection

Water samples were collected at a single fixed station (a floating pontoon extending ~ 10 m into the pond from the shore) in each pond (Leybeek, Pêcheries, Tenreuken, Silex). Sampling occurred on the same day between 9 a.m and 11 a.m., 38 times per pond between January 2022 and December 2023. Sampling frequency was once per month in fall and winter and thrice per month in spring and summer. Water was sampled 5 cm below the surface with 60-ml polypropylene syringes for dissolved CH_4 concentration ($n = 2$) and $^{13}C/^{12}C$ ratio of CH_4 ($\delta^{13}C$-CH_4) ($n = 1$), then transferred via silicone tubing into 60-ml borosilicate serum bottles (Wheaton), preserved with 200 µl of a saturated solution of $HgCl_2$ (70 g L^{-1}), sealed with a butyl stoppers and crimped with aluminium caps, without headspace, and stored at ambient temperature in the dark prior to analysis in the laboratory.

Three bubble traps were deployed 50 cm apart at the same depth (typically along the floating pontoon) to measure the ebullitive CH_4 fluxes reported by Bauduin et al. (2025). Bubble traps were deployed in 2022–2023, twice per pond to cover a temperature gradient; each deployment lasted at least 3 days: Leybeek (5–9 September 2023, $n = 5$; 19–21 October 2023, $n = 3$), Pêcheries (13–17 July 2023, $n = 5$; 11–13 October 2023, $n = 3$), Tenreuken (28–30 October 2023, $n = 3$; 22–25 August 2023, $n = 4$), and Silex (29 March-15 April 2022, $n = 18$; 18–23 July 2022, $n = 6$) ponds. Deployments were in spring, summer, or fall, but not winter, because ebullition is strongly temperature dependent and negligible at low temperature (Aben et al. 2017).

The bubble traps consisted of inverted polypropylene funnels (diameter 23.5 cm) mounted with 60-ml polypropylene syringes and three-way stop valves to collect the gas without ambient air contamination. The funnels were attached with steel rods (length 35 cm) to square polystyrene floats (30 cm × 30 cm) (Fig. S1). The gas collected in the funnels was sampled once per day using graduated 60-ml polypropylene syringes and immediately transferred to pre-evacuated 12-l vials (Exetainers, Labco, UK) and stored at ambient temperature in the dark prior to $\delta^{13}C$–CH_4 analysis in the laboratory.

On 4 September 2023, sediment bubbles were directly collected by perturbing sediments under bubble traps with a wooden stick from pontoons extending ~ 10 m into the ponds. Sampling was performed in triplicate in all four ponds on the same day. Gas collected in the funnels was stored in pre-evacuated 12-ml Exetainers. These samples are henceforth referred to as ‘perturbed sediments’. Samples collected in bubble traps during ebullition measurements are henceforth referred to as ‘trapped bubbles’.

In the Leybeek pond, bubble trap deployment for ebullition measurements began the day after perturbed sediment sampling, allowing comparison between approaches. The mean perturbed-sediment $\delta^{13}C$–CH_4 on 4 September 2023 ($-69.7 \pm 0.7‰$, $n = 3$) was close to the mean trapped-bubble $\delta^{13}C$-CH_4 on 5 September 2023 ($-66.8 \pm 0.4‰$, $n = 3$).

Laboratory analysis

Chl-a, TSM, and dissolved CH_4 concentrations were reported by Bauduin et al. (2025). Chl-a concentration was measured in 90% acetone extracts by fluorimetry (Yentsch and Menzel 1963). TSM was measured by mass difference before and after filtration on 47-mm GF/F grade glass fibre filters. Dissolved CH_4 concentration was measured by the headspace technique (Weiss 1981) using a 20-ml ultra-pure N_2 headspace (Air Liquide Belgium) and a gas chromatograph (SRI 8610C) with flame ionization detector calibrated with CH_4:N_2 mixtures (Air Liquide Belgium) at mixing ratios of 1, 10, and 30 p.p.m., yielding a final precision of ± 3.9%. The $\delta^{13}C$–CH_4 was measured in the headspace gas (20 ml of synthetic air; Air Liquid Belgium) equilibrated with the 40-ml water sample (total volume 60 ml) and directly in the gas stored in Exetainers for bubble samples. Gas samples were diluted to obtain a final CH_4 partial pressure in the cavity < 10 p.p.m. (target 6 p.p.m.) to fall within the operational concentration range of the instrument recommended by the manufacturer, prior to injection into a cavity ring-down spectrometer (G2201-*i* Isotopic Analyzer; Picarro) with a Small Sample Introduction Module 2 (Picarro). Data were corrected using $\delta^{13}C$–CH_4 versus concentration curves based on serial dilutions with synthetic air of two Airgas Specialty Gases standards with certified $\delta^{13}C$–CH_4 values of -23.9 ± 0.3 ‰ and -69.0 ± 0.3 ‰.

CH_4 oxidation

The fraction of oxidized CH_4 (FOX) estimates the fraction of dissolved CH_4 at the sampling moment that was oxidized since its production in sediments. FOX contextualizes dissolved CH_4 concentrations in surface water and helps the interpretation of seasonal and spatial (horizontal or vertical) patterns. MOX is the rate of CH_4 consumption by methanotrophs and can be compared consistently with other CH_4 fluxes such as methanogenesis and emission to the atmosphere.

FOX was calculated with a closed-system Rayleigh fractionation model (Liptay et al. 1998):

$$\ln(1-\text{FOX}) = \frac{\ln\left(\delta^{13}\text{C - CH}_{4\_\text{initial}} + 1000\right) - \ln\left(\delta^{13}\text{C - CH}_4 + 1000\right)}{\alpha - 1}$$

where $\delta^{13}C\text{-}CH_{4\_initial}$ is the $^{13}C/^{12}C$ ratio of dissolved CH_4 produced by sediment methanogenesis, $\delta^{13}C\text{-}CH_4$ is the in-situ $^{13}C/^{12}C$ ratio of dissolved CH_4, and α is the fractionation factor.

We used $\alpha = 1.02$, corresponding to a central value from several studies that report ranges of 1.006–1.028 in culture experiments (Coleman et al. 1981; Templeton et al. 2006; Feisthauer et al. 2011), 1.005–1.026 in soils (forest, grassland, cropland) from eight different studies summarized by Malghani et al. (2016), 1.018–1.021 in the water column of three Swedish lakes (Bastviken et al. 2002), and 1.012–1016 in two tropical lakes (Morana et al. 2015, 2020).

Because $\delta^{13}C\text{-}CH_4$ sampling of dissolved CH_4 was more frequent than sediment bubble sampling, we used seasonal mean bubble-trapped $\delta^{13}C\text{-}CH_4$ values for $\delta^{13}C\text{-}CH_{4-initial}$ across all ponds: − 69‰ for spring and summer, − 83‰ for fall. For winter, we used − 76‰, the average of the fall and spring/summer values. FOX was computed for each individual value of $\delta^{13}C\text{-}CH_4$ of dissolved CH_4 ($n = 38$ for each pond).

MOX (mmol m^{-2} day^{-1}) was computed from FOX and $F_{diff}CH_4$ following Bastviken et al. (2002):

$$\text{MOX} = \text{FdiffCH4} \times \frac{\text{FOX}}{1 - \text{FOX}}$$

$F_{diff}CH_4$ (mmol m^{-2} day^{-1}) was computed as:

$$F_{diff}CH_4 = k\text{x}\ \Delta CH_4$$

where k is the gas transfer velocity and ΔCH_4 is the air–water CH_4 concentration gradient.

k was computed from k_{600} [normalized to a Schmidt number of 600 (cm h^{-1})] and the Schmidt number of CH_4 in fresh water using the temperature function of Wanninkhof (1992). For nominal estimates, k_{600} was calculated with the parameterization of Cole and Caraco (1998) as a function of wind speed (U_{10}) based on tracer experiments in 14 lakes:

$$k_{600} = 2.07 + 0.215\ \text{x}\ U_{10}^{1.7}$$

For sensitivity analysis, we additionally applied the parameterization of MacIntyre et al. (2010) (M10) based on eddy-covariance measurements in Lake Meräsjarvi (Sweden) and Vachon and Prairie (2013) (VP13) based on floating chamber measurements in Eastmain-1 reservoir (Canada):

$$\text{M10}: k_{600} = 0.16 + 2.25\ \text{x}\ U_{10}$$

$$\text{VP13}: k_{600} = 1.62 + 2.78\ \text{x}\ U_{10}$$

Daily U_{10} means were retrieved from https://wow.meteo.be/en for the Royal Meteorological Institute station at St-Lambert (50.8408°N, 4.4234°E), 2.5–5.0 km from the ponds. ΔCH_4 was computed from measured dissolved CH_4 concentration by gas chromatography (see above) and the equilibrium concentration derived from the global average present-day atmospheric mixing ratio of 1.9 p.p.m. (Lan et al. 2024). Henry's constant was computed from water temperature by using the formulation of Yamamoto et al. (1976).

The CH_4 flux from the dissolution of rising bubbles was computed using the McGinnis et al. (2006) model implemented in the SiBu-GUI interface (Greinert and McGinnis 2009).

Statistical analysis

Group comparisons were conducted in GraphPad Prism using $\log_{10}$-transformed data. Data normality was assessed with the Shapiro–Wilk test, and the results are summarized in Table S1.

ANOVA with the Tukey honestly significant difference post hoc test was used to test differences in means of (i) $\delta^{13}C\text{-}CH_4$ in dissolved water, FOX, MOX, Chl-a, and TSM among four seasons (spring, summer, fall, winter) in individual pond (Leybeek, Pêcheries, Tenreuken, and Silex); (ii) $\delta^{13}C\text{-}CH_4$ in dissolved water, FOX, MOX among ponds (Leybeek, Pêcheries, Tenreuken, and Silex) all four seasons merged; (iii) MOX (ponds and four seasons merged) between nominal and alternative calculations using two other k_{600} parameterizations (M10 and VP13) or fixed $\delta^{13}C\text{-}CH_{4\_initial}$ values (− 69‰ and − 83‰); (iv) all dissolved CH_4 fluxes (bubble dissolution flux, MOX, $F_{diff}CH_4$, and sedimentary diffusive CH_4 flux) in individual ponds (Leybeek, Pêcheries, Tenreuken, and Silex), all four seasons merged.

The Kruskal–Wallis test with Dunn's multiple comparisons test was used to test differences in means of bubble-trapped $\delta^{13}C\text{-}CH_4$ (all ponds merged) between three seasons (spring, summer, and fall). The Mann–Whitney test was used to test differences of medians of (i) bubble-trapped $\delta^{13}C\text{-}CH_4$ between two seasons (summer versus fall; spring versus summer) in individual ponds (Leybeek, Pêcheries,

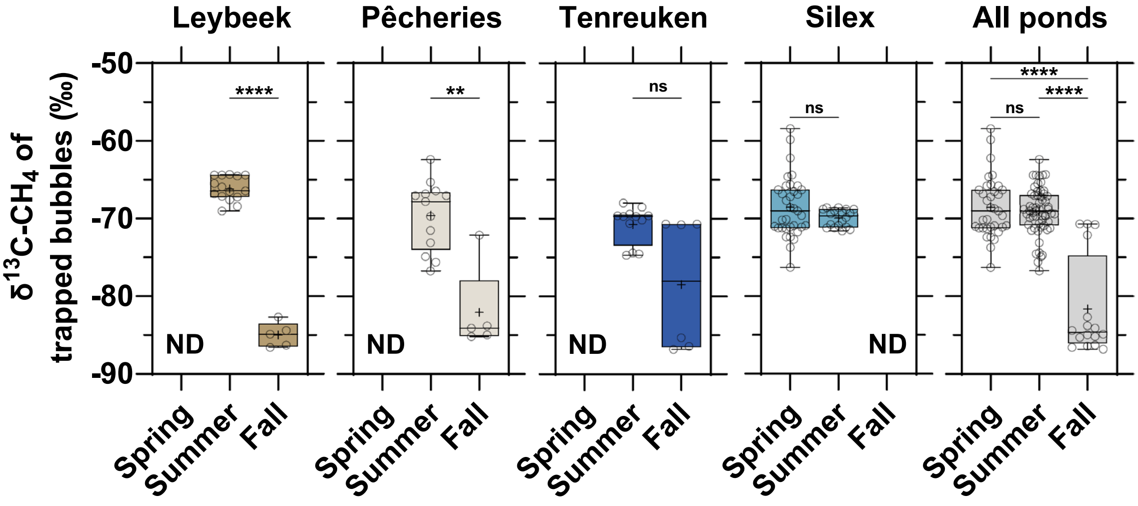

Fig. 2 $^{13}C/^{12}C$ ratio of CH_4 ($\delta^{13}C$-CH_4) in bubbles collected during ebullitive flux measurements (*trapped bubbles*) in four urban ponds (Leybeek, Pêcheries, Tenreuken, and Silex) in the city of Brussels (Belgium), measured in spring, summer, and fall in 2022 and 2023 (September 2023 and October 2023 in the Leybeek pond; July 2023 and October 2023 in the Pêcheries pond; August 2023 and October 2023 in the Tenreuken pond; April 2022 and July 2022 in the Silex pond). Box plots show median (*horizontal line*), mean (*cross*), and 25–75% percentiles (*box limits*). *Whiskers* extend from minimum to maximum values. Results of the statistical comparison of means/medians are summarized at the top of the figures and detailed in Tables S2 and S3, respectively. *ND* No data

Tenreuken, and Silex); (ii) perturbed-sediment $\delta^{13}C$-CH_4 between turbid-water (Leybeek + Pêcheries) and clear-water (Tenreuken + Silex) ponds.

Quantile regressions were computed from the median (*tau* = 0.5) with the quantreg package (Koenker 2005) in R (R Core Team 2022).

Results and discussion

Methanogenesis pathway inferred from $\delta^{13}C$-CH_4 in bubbles

We measured $\delta^{13}C$-CH_4 in trapped bubbles (ebullition measurements; Table 1) and in bubbles released by sediment perturbation in four ponds in the city of Brussels (Leybeek, Pêcheries, Tenreuken, Silex). Across the full dataset, trapped-bubble $\delta^{13}C$-CH_4 values were significantly more negative in fall (– 83.2 ± 5.2 ‰) than in summer (– 69.5 ± 3.2 ‰) and spring (– 68.2 ± 4.4 ‰) (Fig. 2; Table S3). Within individual ponds, trapped-bubble $\delta^{13}C$-CH_4 values were significantly higher in summer in the Leybeek and the Pêcheries ponds, but not significantly different in the Tenreuken pond (Fig. 2; Table S2). These trapped-bubble $\delta^{13}C$-CH_4 seasonal changes suggest seasonal variation in the relative importance of hydrogenotrophic versus acetoclastic pathways of methanogenesis. Hydrogenotrophic methanogenesis produces CH_4 with more negative $\delta^{13}C$ (– 100‰ to -60‰) compared to acetoclastic methanogenesis (– 65‰ to – 50‰) (Whiticar et al. 1986). Thus, the observed seasonal trapped-bubble $\delta^{13}C$-CH_4 pattern suggests greater importance of hydrogenotrophic methanogenesis in fall relative to spring and summer, when acetoclastic methanogenesis appeared more important. The environmental drivers controlling the relative importance of these pathways remain unclear (Conrad et al. 2011). Hydrogenotrophic methanogenesis has been reported to occur at higher temperatures than acetoclastic methanogenesis (Schulz and Conrad 1996; Schulz et al. 1997), but mean fall temperature (11.9 ± 3.7 °C) was lower than mean

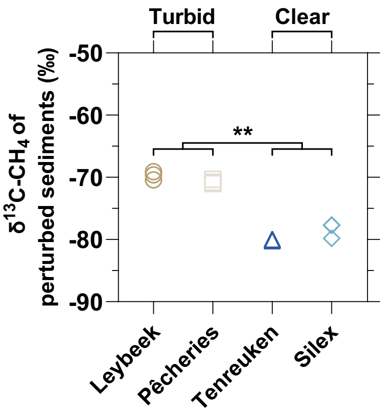

Fig. 3 Stacked measurements ($n = 3$) of $\delta^{13}C$-CH_4 in bubbles released from sediments after physical perturbation (*perturbed sediments*) in four ponds (Leybeek, Pêcheries, Tenreuken, and Silex) in the city of Brussels (Belgium) on 4 September 2023. Results of the statistical comparison of medians of turbid (Leybeek and Pêcheries) and clear-water (Tenreuken and Silex) ponds are summarized at the top of the figure and detailed in Table S2

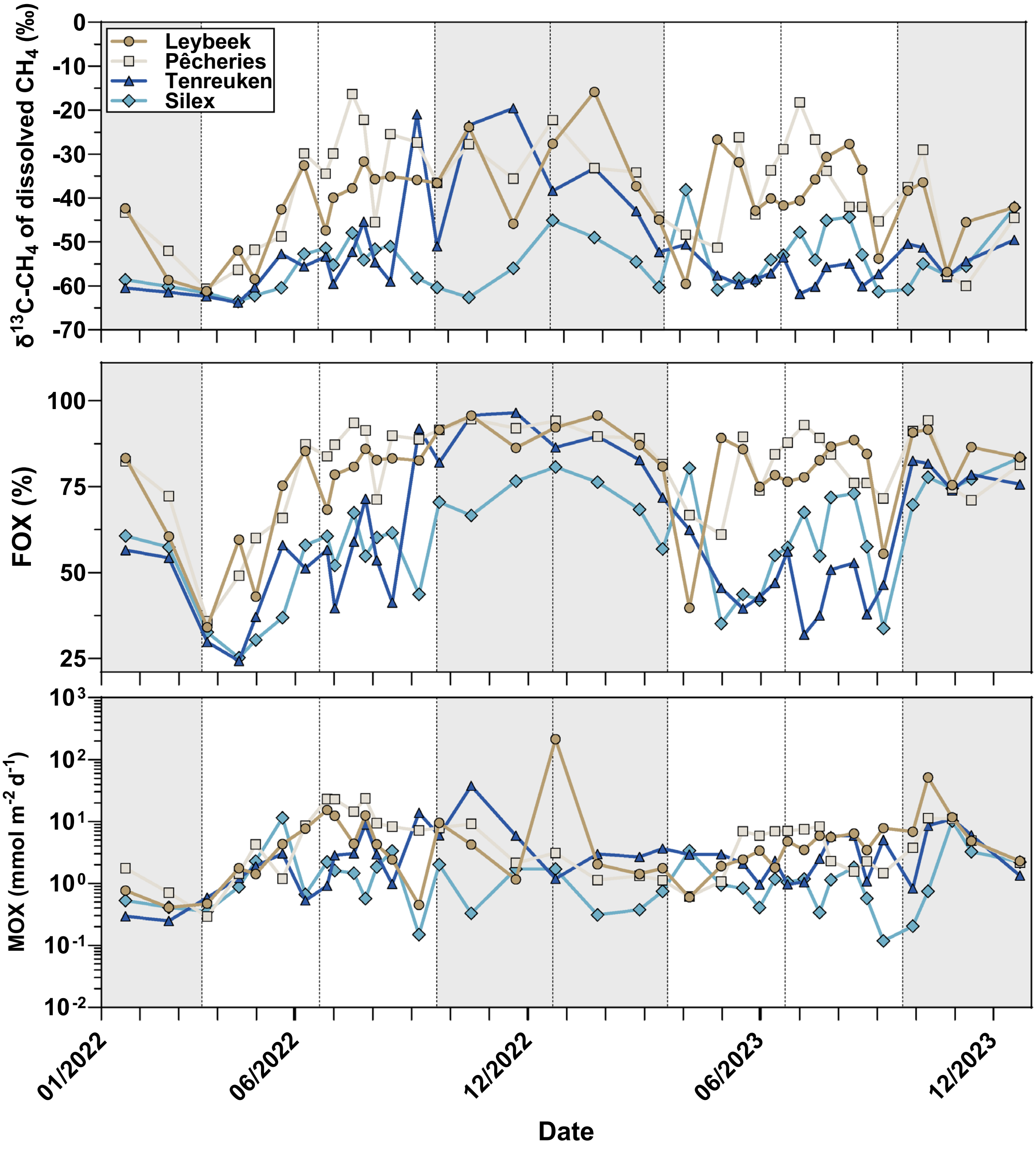

Fig. 4 Seasonal variations of δ^{13}C-CH$_4$ of dissolved CH$_4$ in surface waters, fraction of dissolved concentration (*FOX*) and rate of CH$_4$ removed by oxidation (*MOX*) in four urban ponds (Leybeek, Pêcheries, Tenreuken, and Silex) in the city of Brussels (Belgium) from January 2022 to December 2023. *White bands* and *grey bands* correspond to the fall/winter and spring/summer periods, respectively, and *dotted vertical lines* represent the first days of each season

summer temperature (21.1 ± 1.9 °C) (Fig. S2). A shift from acetoclastic to hydrogenotrophic methanogenesis has been observed in soils in response to increased NH$_4^+$ concentration (Ni et al. 2022; Wang et al. 2022) and decreased pH (Kotsyurbenko et al. 2007) expected with an increase of CO$_2$. An increase of NH$_4^+$ and decrease of pH in the ponds' sediment pore waters from spring to fall driven by sustained benthic organic matter degradation, following the cycle of aquatic primary production, would be consistent with the observed shift in the methanogenesis pathway.

In summer 2023, we simultaneously sampled perturbed-sediment bubbles across all four ponds to compare δ^{13}C-CH$_4$ values. Perturbed-sediment δ^{13}C-CH$_4$ were significantly (p = 0.002) lower in the clear-water macrophyte-dominated ponds (− 80.1 ± 0.1 ‰ and − 78.4 ± 1.2 ‰ for the Tenreuken and Silex ponds, respectively) than in the turbid-water

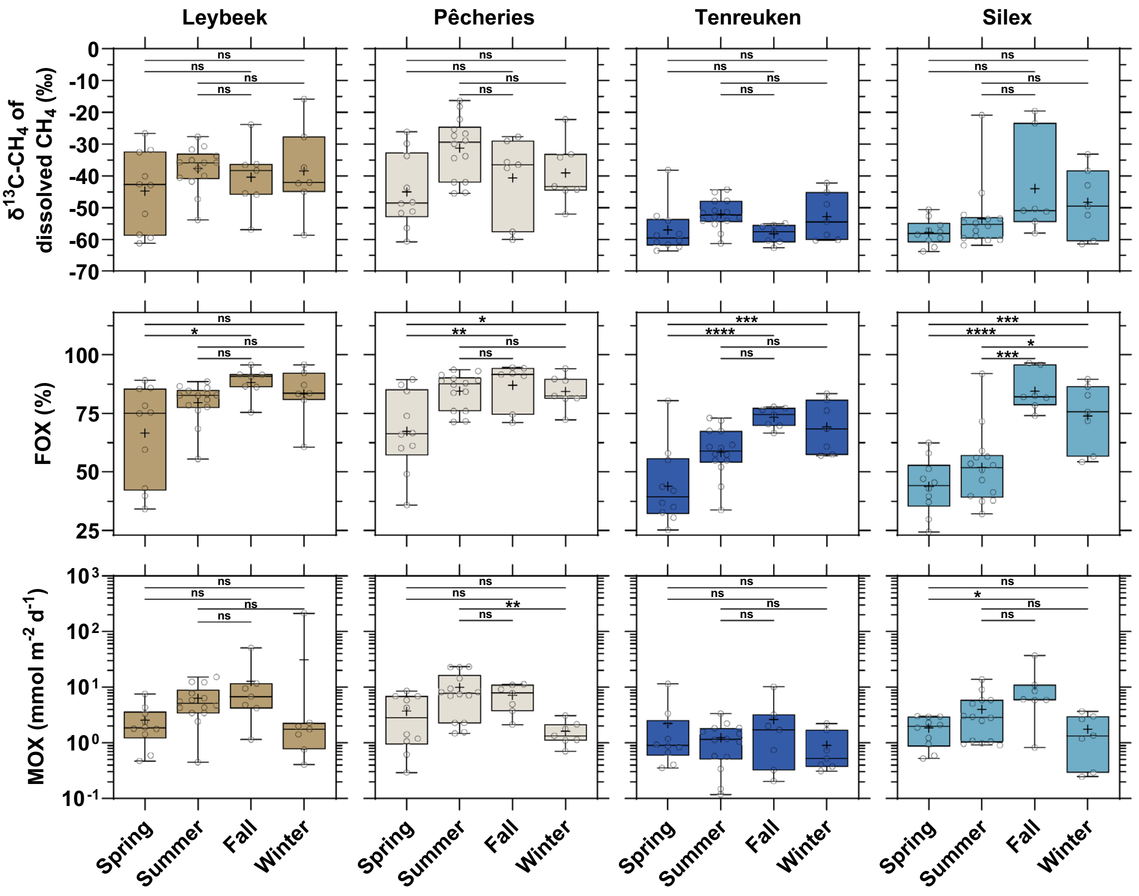

Fig. 5 Box plots per season of δ^{13}C-CH$_4$ of dissolved CH$_4$ in surface waters, FOX and MOX in four urban ponds (Leybeek, Pêcheries, Tenreuken, and Silex) in the city of Brussels (Belgium) from January 2022 to December 2023. Box plots show median (*horizontal line*), mean (*cross*), and 25–75% percentiles (*box limits*). *Whiskers* extend from minimum to maximum values. Results of the statistical comparison of means are summarized at the top of the figures and detailed in Table S4. For abbreviations, see Figs. 2 and 4

phytoplankton-dominated ponds (− 69.7 ± 0.7 ‰ and − 70.7 ± 0.4 ‰ for the Leybeek and Pêcheries ponds, respectively) (Fig. 3; Table S2). Two explanations may account for this pattern: at the moment of sampling, perturbed-sediment δ^{13}C-CH$_4$ in the macrophyte-dominated ponds (Tenreuken and Silex) reflected fall-like conditions based on the bubble-trapped data (Fig. 2), whereas perturbed-sediment δ^{13}C-CH$_4$ in phytoplankton-dominated ponds (Leybeek and Pêcheries) reflected summer conditions; or the perturbed-sediment δ^{13}C-CH$_4$ differences reflect distinct methanogenic pathways driven by differing organic matter sources (phytoplankton versus macrophyte). The latter would imply a higher contribution of hydrogenotrophic methanogenesis in clear-water ponds where sediment organic matter is presumably primarily macrophyte derived. Based on gene expression during incubations, Wang et al. (2023) suggested acetoclastic methanogenesis was stimulated by macrophyte organic carbon compared to phytoplankton in lakes Chaohu and Taihu (China). Our δ^{13}C-CH$_4$ data distribution across the four Brussels' ponds suggests the opposite: macrophyte organic carbon stimulating hydrogenotrophic methanogenesis. This pattern aligns with the more refractory nature of macrophyte organic matter relative to more labile phytoplankton organic carbon (Grasset et al. 2018). Macrophyte-derived organic matter contains a large proportion of recalcitrant molecules, such as cellulose, whereas phytoplankton organic matter is rich in polysaccharides and proteins (West et al. 2012; Berberich et al. 2020). When organic matter is more refractory, partial fermentation favours H$_2$ production over acetate, which would favour hydrogenotrophic over acetoclastic methanogenesis (Liu et al. 2017).

CH$_4$ oxidation

The δ^{13}C-CH$_4$ of dissolved CH$_4$ in surface water samples in the four ponds ranged from − 16 ‰ to − 64 ‰ (Fig. 4). These values were enriched in ^{13}C relative to trapped-bubble values (− 55 ‰ to − 87 ‰; Fig. 2), consistent with isotopic enrichment from MOX. FOX in surface water samples ranged from 22 to 97%, and MOX ranged from 0.1

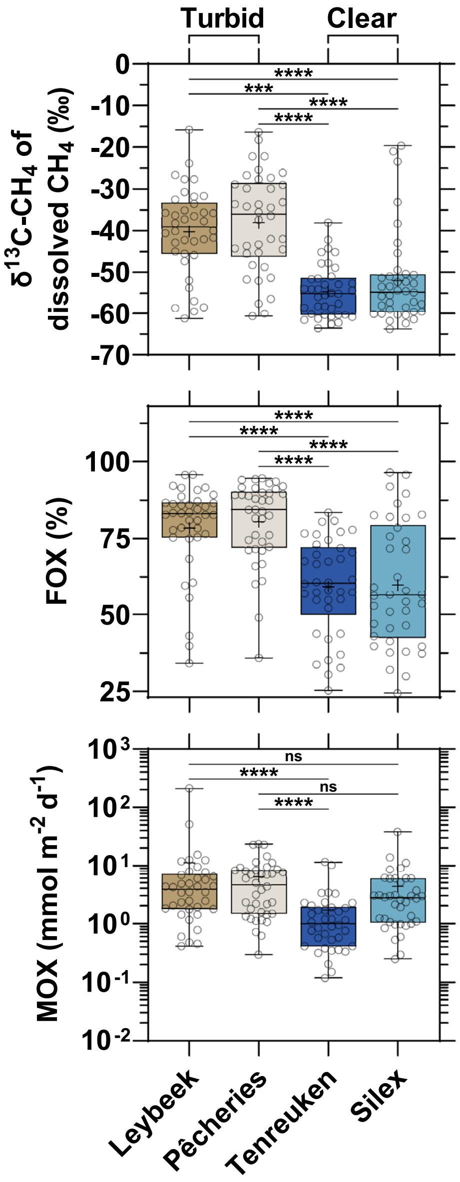

Fig. 6 Box plots per pond of δ^{13}C-CH$_4$ of dissolved CH$_4$ in surface waters, FOX and MOX in four urban ponds (Leybeek, Pêcheries, Tenreuken, and Silex) in the city of Brussels (Belgium) from January 2022 to December 2023. Box plots show median (*horizontal line*), mean (*cross*), and 25–75% percentiles (*box limits*). *Whiskers* extend from minimum to maximum values. Results of the statistical comparison of means are summarized at the top of the figures and detailed in Table S4. For abbreviations, see Fig. 2 and 4

to 73.0 mmol m^{-2} day^{-1} (Fig. 4). Because FOX and MOX were derived from the same isotopic model, their spatial and temporal patterns mirrored those of δ^{13}C-CH$_4$ of dissolved CH$_4$ in surface water.

Within individual ponds, δ^{13}C-CH$_4$ of dissolved CH$_4$, FOX, and MOX did not show significant seasonal variations, except FOX in the two clear-water ponds (Silex and Tenreuken) (Fig. 5; Table S4). In the Silex pond, FOX in fall and winter was significantly higher than in spring and summer (Fig. 5; Table S4). In the Tenreuken pond, FOX in fall and winter was significantly higher than in spring, but not significantly different from summer (Fig. 5; Table S4). These seasonal FOX differences might reflect increased Chl-a and TSM concentrations in fall and winter relative to spring and summer (see hereafter) in these two clear-water ponds (Fig. S3; Table S4), presumably due to sediment resuspension (Bauduin et al. 2025). However, these FOX seasonal differences in Silex and Tenreuken did not translate into significant seasonal differences in MOX rates in any pond (Fig. 5; Table S4).

δ^{13}C-CH$_4$ of dissolved CH$_4$ and FOX were significantly higher in the two turbid-water ponds (Leybeek and Pêcheries) than the two clear-water ponds (Silex and Tenreuken) (Fig. 6; Table S4). MOX was significantly higher in the two turbid-water ponds (Leybeek and Pêcheries) than in one of the clear-water ponds (Tenreuken), but not significantly different from the Silex clear-water pond (Fig. 6; Table S4). These differences of means of δ^{13}C-CH$_4$ of dissolved CH$_4$, FOX, and MOX among the four ponds were consistent, with significant positive relationships between these quantities and Chl-a and TSM (Fig. 7; Table S5). These positive relationships may reflect the increase of abundance of particle-attached methanotrophs with higher TSM, as shown in rivers (Abril et al. 2007). Attached microorganisms can colonize inorganic particles, aggregates of detrital organic matter (Kirchman and Mitchell 1982), and aggregates of living cyanobacteria (Li et al. 2021). Increased particle load in the water column attenuates light, alleviating MOX inhibition by light (Dumestre et al. 1999; Murase and Sugimoto 2005; Morana et al. 2020), which may further contribute to higher MOX with rising TSM and Chl-a along the turbidity gradient, from clear- to turbid-water ponds. Both increased particle-attached methanotroph abundance and reduced light inhibition likely co-occur, explaining the observed positive relationships between MOX and TSM/Chl-a (Fig. 7).

Limitations of modelled MOX

We assessed uncertainty in MOX estimates from the isotopic fractionation model arising from α, δ^{13}C–CH$_{4\_initial}$, and k_{600}. We used a constant $\alpha = 1.02$, informed by culture studies (Coleman et al. 1981; Templeton et al. 2006; Feisthauer et al. 2011), soil field measurements (Malghani et al. 2016), and lake studies (Bastviken et al. 2002; Morana et al. 2015, 2020). In landfills, α was found to be temperature dependent, decreasing with temperature (− 0.00039 °C^{-1}) (Chanton et al. 2008). Conversely, Bastviken et al. (2002) reported season- and temperature-independent α values in three Swedish lakes. Propagating an α error of ± 0.005 produced

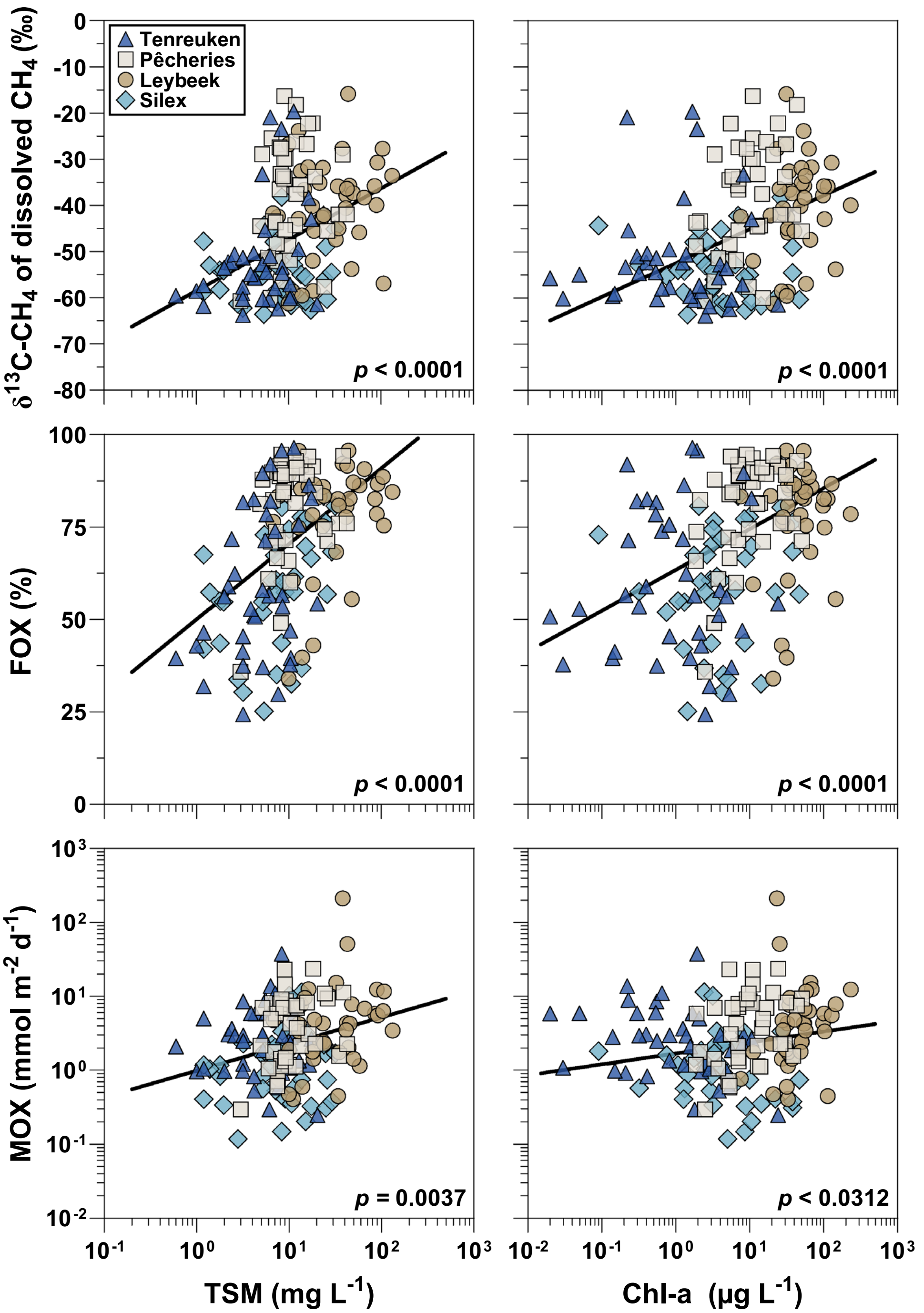

Fig. 7 δ^{13}C-CH$_4$ of dissolved CH$_4$ in surface waters, FOX and MOX versus total suspended matter concentration (*TSM*) and chlorophyll-*a* concentration (*Chl-a*) in four urban ponds (Leybeek, Pêcheries, Tenreuken, and Silex) in the city of Brussels (Belgium) from January 2022 to December 2023. *Black lines* indicate quantile linear regressions (Table S5). For other abbreviations, see Figs. 2 and 4

estimated uncertainties of ± 6.5% and ± 28.7% for FOX and MOX, respectively, in our dataset.

We used seasonal varying δ^{13}C-CH$_{4\_initial}$ based on bubble trap measurements (− 83 to − 69‰), within the range reported in freshwater sediments (Schenk et al. 2021; Balathandayuthabani et al. 2024), to derive nominal MOX estimates. Recomputing MOX using fixed δ^{13}C-CH$_{4\_initial}$ values for the whole year gave mean MOX of 4.3 ± 12.0 mmol m^{-2} day^{-1} for a constant − 69‰ (1.35-fold lower than the nominal 5.9 ± 18.1 mmol m^{-2} day^{-1}) and 11.1 ± 27.4 mmol m^{-2} day^{-1} for a constant − 83‰ (1.89-fold higher than the nominal value); the latter difference was significant (Fig. 8; Table S4).

Nominal MOX computations were made using the Cole and Caraco (1998) k_{600} parameterization. The nominal mean MOX (5.9 ± 18.1 mmol m^{-2} day^{-1}) was 1.66-fold higher than that computed with MacIntyre et al. (2010) (3.5 ± 11.4 mmol m^{-2} day^{-1}) and 1.39-fold lower than with Vachon and Prairie (2013) (8.2 ± 25.5 mmol m^{-2} day^{-1}) k_{600}

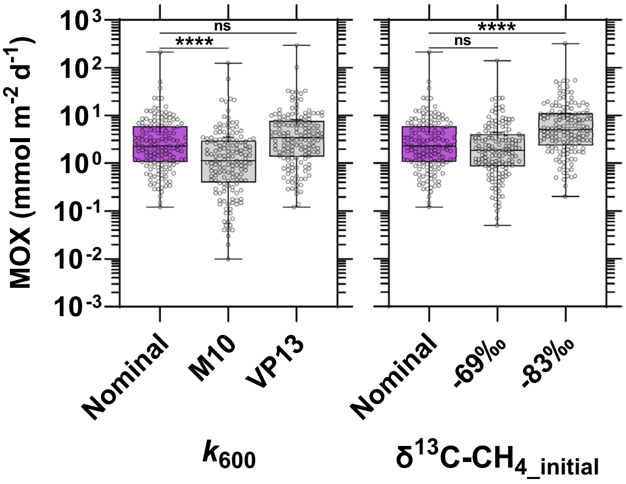

Fig. 8 Comparison of CH_4 oxidation (*MOX*) computed with an isotopic fractionation model with nominal choices of gas transfer velocity (k_{600}) and of initial $\delta^{13}C\text{-}CH_4$ ($\delta^{13}C\text{-}CH_{4\_initial}$) versus alternative k_{600} and $\delta^{13}C\text{-}CH_{4\_initial}$ values. The Cole and Caraco (1998) k_{600} parameterization was used nominally, while the MacIntyre et al. (2010) (*M10*) and Vachon and Prairie (2013) parameterizations (*VP13*) were used as alternatives. Different values of $\delta^{13}C\text{-}CH_{4\_initial}$ were used per season nominally (-69‰ for spring and summer, -83‰ for fall, -76‰ for winter), while fixed values for all seasons (− 69 and − 83‰) were used as alternatives. Results of the paired statistical comparison of means are summarized at the top of the figures and detailed in Table S4

parameterizations, although the latter difference was not significant (Fig. 8; Table S4).

This sensitivity analysis highlighted the need to quantify the error from using a constant α, as done here and in other lake studies (Bastviken et al. 2002). A constant α reflects limited lake data to develop a more elaborate approach (e.g. including temperature dependence). Choice of $\delta^{13}C\text{-}CH_{4\_initial}$ values and k_{600} parameterization exerted a larger impact on MOX estimates than α uncertainty. To model MOX reliably using isotopic fractionation, $\delta^{13}C\text{-}CH_{4\_initial}$ should be determined from sediment gas or pore water measurements in addition to dissolved $\delta^{13}C\text{-}CH_4$ in the water column, because $\delta^{13}C\text{-}CH_{4\_initial}$ may vary seasonally, as observed here. Selecting a k_{600} parameterization from U_{10} is challenging (Klauss and Vachon 2020). We used Cole and Caraco (1998) for nominal computations because it was derived from deliberate tracer estimates in 14 lakes spanning a wide depth (1–109 m) and surface area range (0.2–487 km^2), thus implicitly integrating other turbulence sources (e.g. nighttime convection) and fetch limitation. Computed k_{600} values for our ponds using Cole and Caraco (1998) ranged from 2.1 to 3.5 cm h^{-1}, and the mean (2.2 ± 0.3 cm h^{-1}) fell within the 0.9–3.0 cm h^{-1} range reported by Holgerson et al. (2017) for four small ponds (~ 0.02 ha). Within our U_{10} range (0–3 m s^{-1}), MacIntyre et al. (2010) yielded a lower mean k_{600} (1.6 ± 1.6 cm h^{-1}) than Cole and Caraco (1998) because of a lower *y*-intercept (0.16 versus 2.07 cm h^{-1}), though at higher U_{10} the higher slope in MacIntyre et al. (2010) produces larger k_{600}.

Budget of dissolved CH_4 fluxes

Figure 9 compiles mean dissolved CH_4 fluxes in the four ponds: MOX, $F_{diff}CH_4$, bubble dissolution, and the sedimentary diffusive CH_4 flux computed as a closing term

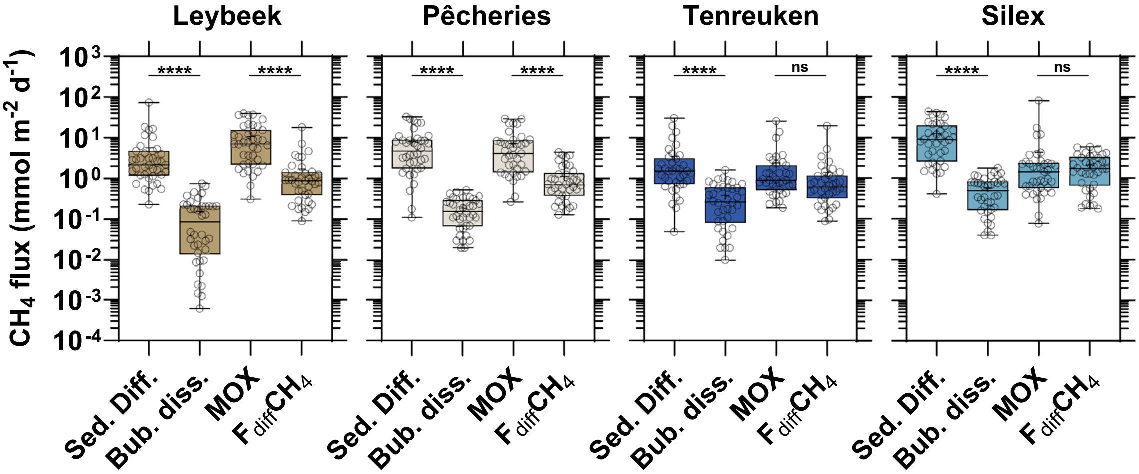

Fig. 9 Bubble dissolution flux (*Bub. Diss.*), CH_4 oxidation (*MOX*), diffusive CH_4 emissions to atmosphere ($F_{diff}CH_4$), and sedimentary diffusive CH_4 flux (*Sed. Diff.*) computed from the other fluxes assuming steady state (= MOX—Bub. Diss. + $F_{diff}CH_4$) in four urban ponds (Leybeek, Pêcheries, Tenreuken, and Silex) in the city of Brussels (Belgium) between June 2021 and December 2023. Box plots show median (*horizontal line*), mean (*cross*), and 25–75% percentiles (*box limits*). *Whiskers* extend from minimum to maximum values. Results of the statistical comparison of means are summarized at the top of the figures and detailed in Table S4

(assuming a steady state). Mean bubble dissolution (0.2 ± 0.2 to 0.6 ± 0.4 mmol m^{-2} day^{-1}) was significantly smaller than the diffusive sedimentary flux (3.4 ± 6.0 to 12.6 ± 12.1 mmol m^{-2} day^{-1}) in each pond. Mean diffusive sedimentary flux was 88 ± 18% of the total dissolved CH_4 input to the water column across ponds (Fig. 9; Table S4). The low contribution of bubble dissolution results from pond shallowness because bubble dissolution depends on ascent time, which scales with depth (McGinnis et al. 2006). In the turbid-water ponds (Leybeek and Pêcheries), MOX was a significantly larger sink of dissolved CH_4 than $F_{diff}CH_4$, representing 80 ± 19% and 80 ± 14% of total dissolved CH_4 removal, respectively (Fig. 9; Table S4). In the clear-water ponds (Tenreuken and Silex), MOX did not significantly differ from $F_{diff}CH_4$ and accounted for roughly half of dissolved CH_4 removal (59 ± 21% and 51 ± 27%, respectively). Across all ponds, MOX accounted for 66 ± 26% of total dissolved CH_4 removal, consistent with other lentic studies (Kankaala et al. 2006; Bastviken et al. 2008; Morana et al. 2020; Reis et al. 2022).

Conclusions

Continued eutrophication will likely increase CH_4 emissions from lakes and ponds (Davidson et al. 2018) and promote the transition from clear- to turbid-water states. Our results indicate that such a transition will likely increase MOX, as evidenced by positive relationships between MOX rates and Chl-a. Increased MOX in eutrophic, turbid ponds will alter pond CH_4 budgets: MOX represented the largest fraction of dissolved CH_4 removal (MOX plus atmospheric emission), corresponding to ~ 80% in the turbid-water ponds and 50–60% in the clear-water ponds. Enhanced MOX in turbid ponds may partly explain why diffusive CH_4 emissions did not differ significantly between clear- and turbid-water ponds in the sampled dataset (Bauduin et al. 2025). Eutrophication will also likely alter sediment microbial community structure (Han et al. 2020), including methanogens (Yang et al. 2020; Bosco-Santos et al. 2025). We documented likely shifts in the relative importance of methanogenic pathways (acetoclastic versus hydrogenotrophic) among pond types and seasonally: in summer, hydrogenotrophic methanogenesis was likely more important in the two clear-water ponds than in the two turbid-water ponds. Acetoclastic methanogenesis was likely more important in spring–summer than fall, across the dataset. We could not identify the exact drivers of these shifts, but we suggest several plausible explanations, including organic matter origin (phytoplankton versus macrophyte) and pore water chemistry (pH and NH_4^+). The dynamic spatial and seasonal changes in the methanogenic pathway suggested here by $\delta^{13}C$-CH_4 data in shallow ponds contrast with evidence from profundal lake sediments, which appear to exhibit more stable methanogenic pathways (Su et al. 2025). This contrast may reflect fundamental differences between shallow and deep lakes in physical and ecological stability (Vicente et al. 2006; Scheffer and van Nes 2007). Such a working hypothesis deserves to be verified by additional measurements of $\delta^{13}C$-CH_4 in sediment bubbles.

Supplementary Information The online version contains supplementary material available at https://doi.org/10.1007/s00027-025-01263-2.

Acknowledgements We thank Ozan Efe (University of Liège) for analytical assistance.

Author contributions AVB and NG designed the experiment. TB collected the samples. AVB supervised the lab analysis, interpreted the data, and wrote the manuscript.

Funding TB received funding from the Institute for the Encouragement of Scientific Research and Innovation (Innoviris) of the Brussels-Capital Region as part of the Smartwater project (RBC/2020-EPF-6 h) and from the Fonds pour la formation à la Recherche dans l'Industrie et dans l'Agriculture" (FRIA, Belgium). The Picarro G2201-*i* isotopic analyzer was funded by the Fund for Scientific Research (FRS-FNRS) (U.N005.21). AVB is a research director at FRS-FNRS.

Data availability The full dataset is available at https:/zenodo.org/records/11103557.

Declarations

Conflict of interest The authors declare no competing interests.

References

Aben RCH, Barros N, van Donk E, Frenken T, Hilt S, Kazanjian G, Lamers LPM, Peeters ETHM, Roelofs JGM, de Senerpont Domis LN, Stephan S, Velthuis M, de Van Waal DB, Wik M, Thornton BF, Wilkinson J, DelSontro T, Kosten S (2017) Cross continental increase in methane ebullition under climate change. Nat Commun 8:1682. https://doi.org/10.1038/s41467-017-01535-y

Abril G, Commarieu MV, Guérin F (2007) Enhanced methane oxidation in an estuarine turbidity maximum. Limnol Oceanogr 52(1):470–475. https://doi.org/10.4319/lo.2007.52.1.0470

Achtnich C, Bak F, Conrad R (1995) Competition for electron donors among nitrate reducers, ferric iron reducers, sulfate reducers, and methanogens in anoxic paddy soil. Biol Fertil Soils 19:65–72. https://doi.org/10.1007/BF00336349

Balathandayuthabani S, Panneer Selvam B, Gålfalk M, Saetre P, Peura S, Kautsky U, Klemedtsson L, Arunachalam L, Vellingiri G, Bastviken D (2024) Methane in two stream networks: similar contributions from groundwater and local sediments while oxidation was a large sink controlling atmospheric emissions. J Geophys Res Biogeosci 129:e2023JG007836. https://doi.org/10.1029/2023JG007836

Bastviken D, Ejlertsson J, Tranvik L (2002) Measurement of methane oxidation in lakes: a comparison of methods. Environ Sci Technol 36:3354–3361. https://doi.org/10.1021/es010311p

Bastviken D, Cole JJ, Pace ML, Van de Bogert MC (2008) Fates of methane from different lake habitats: connecting whole-lake budgets and CH_4 emissions. J Geophys Res Biogeosci. https://doi.org/10.1029/2007JG000608

Bauduin T, Gypens N, Borges AV (2024) Seasonal and spatial variations of greenhouse gas (CO_2, CH_4 and N_2O) emissions from urban ponds in Brussels. Water Res 253:121257. https://doi.org/10.1016/j.watres.2024.121257

Bauduin T, Gypens N, Borges AV (2025) Methane, carbon dioxide, and nitrous oxide emissions from two clear-water and two turbid-water urban ponds in Brussels (Belgium). Biogeosciences 22:3785–3805. https://doi.org/10.5194/bg-22-3785-2025

Berberich ME, Beaulieu JJ, Hamilton TL, Waldo S, Buffam I (2020) Spatial variability of sediment methane production and methanogen communities within a eutrophic reservoir: importance of organic matter source and quantity. Limnol Oceanogr 65:1–23. https://doi.org/10.1002/lno.11392

Borrel G, Jézéquel D, Biderre-Petit C, Morel-Desrosiers N, Morel J-P, Peyret P, Fonty G, Lehours A-C (2011) Production and consumption of methane in freshwater lake ecosystems. Res Microbiol 162:832–847. https://doi.org/10.1016/j.resmic.2011.06.004

Bosco-Santos A, Beyala Bekono ER, Khatun S, Monchamp M-È, Séneca J, Pjevac P, Berg JS (2025). Imprint of eutrophication on methane-cycling microbes in freshwater sediment, Preprint egusphere-2025-4489, https://doi.org/10.5194/egusphere-2025-4489.

Bosse U, Frenzel P, Conrad R (1993) Inhibition of methane oxidation by ammonium in the surface layer of a littoral sediment. FEMS Microbiol Ecol 13:123–134. https://doi.org/10.1016/0168-6496(93)90030-B

Cabrera-Lamanna L, Marquina-Luevano I, Visser EJW, van Oevelen D, Lorke A, Kosten S (2025) Rooted macrophytes reduce sediment CH_4storage and net production: an experimental approach using a novel scanning method. Limnol Oceanogr Lett. https://doi.org/10.1002/lol2.70073

Chanton JP, Powelson DK, Abichou T, Fields D, Green R (2008) Effect of temperature and oxidation rate on carbon-isotope fractionation during methane oxidation by landfill cover materials. Environ Sci Technol 42:7818–7823. https://doi.org/10.1021/es801221y

Cole JJ, Caraco NF (1998) Atmospheric exchange of carbon dioxide in a low-wind oligotrophic lake measured by the addition of SF6. Limnol Oceanogr 43:647–656. https://doi.org/10.4319/lo.1998.43.4.0647

Coleman DD, Risatti JB, Schoell M (1981) Fractionation of carbon and hydrogen isotopes by methane oxidizing bacteria. Geochim Cosmochim Acta 45:1033–1037. https://doi.org/10.1016/0016-7037(81)90129-0

Conrad R (1999) Contribution of hydrogen to methane production and control of hydrogen concentrations in methanogenic soils and sediments. FEMS Microbiol Ecol 28:193–202. https://doi.org/10.1111/j.1574-6941.1999.tb00575.x

Conrad R, Noll M, Claus P, Klose M, Bastos WR, Enrich-Prast A (2011) Stable carbon isotope discrimination and microbiology of methane formation in tropical anoxic lake sediments. Biogeosciences 8(3):795–814. https://doi.org/10.5194/bg-8-795-2011

Davidson TA, Audet J, Jeppesen E, Landkildehus F, Lauridsen TL, Søndergaard M, Syväranta J (2018) Synergy between nutrients and warming enhances methane ebullition from experimental lakes. Nat Clim Change 8:156–160. https://doi.org/10.1038/s41558-017-0063-z

Davidson TA, Sayer CD, Jeppesen E, Søndergaard M, Lauridsen TL, Johansson LS, Baker A, Graeber D (2023) Bimodality and alternative equilibria do not help explain long-term patterns in shallow lake chlorophyll-a. Nat Commun 14:398. https://doi.org/10.1038/s41467-023-36043-9

De Backer S, Van Onsem S, Triest L (2010) Influence of submerged vegetation and fish abundance on water clarity in peri-urban eutrophic ponds. Hydrobiologia 656:255–267. https://doi.org/10.1007/s10750-010-0444-z

Duc NT, Crill P, Bastviken D (2010) Implications of temperature and sediment characteristics on methane formation and oxidation in lake sediments. Biogeochemistry 100:185–196. https://doi.org/10.1007/s10533-010-9415-8

Dumestre JF, Guézennec J, Galy-Lacaux C, Delmas R, Richard S, Labroue L (1999) Influence of light intensity on methanotrophic bacterial activity in Petit Saut reservoir, French Guiana. Appl Environ Microbiol 65:534–539. https://doi.org/10.1128/aem.65.2.534-539.1999

Durisch-Kaiser E, Schmid M, Peeters F, Kipfer R, Dinkel C, Diem T, Schubert CJ, Wehrli B (2011) What prevents outgassing of methane to the atmosphere in Lake Tanganyika? J Geophys Res 116:G02022. https://doi.org/10.1029/2010JG001323

Feisthauer S, Vogt C, Modrzynski J, Szlenkier M, Krüger M, Siegert M, Richnow H-H (2011) Different types of methane monooxygenases produce similar carbon and hydrogen isotope fractionation patterns during methane oxidation. Geochim Cosmochim Acta 75:1173–1184. https://doi.org/10.1016/j.gca.2010.12.006

Grasset C, Mendonça R, Villamor Saucedo G, Bastviken D, Roland F, Sobek S (2018) Large but variable methane production in anoxic freshwater sediment upon addition of allochthonous and autochthonous organic matter. Limnol Oceanogr 63:1488–1501. https://doi.org/10.1002/lno.10786

Greinert J, McGinnis DF (2009) Single bubble dissolution model—the graphical user interface SiBu-GUI. Environ Model Softw 24:1012–1013. https://doi.org/10.1016/j.envsoft.2008.12.011

Han X, Schubert CJ, Fiskal A, Dubois N, Lever MA (2020) Eutrophication as a driver of microbial community structure in lake sediments. Environ Microbiol 22:3446–3462. https://doi.org/10.1111/1462-2920.15115

Holgerson MA, Farr ER, Raymond PA (2017) Gas transfer velocities in small forested ponds. J Geophys Res Biogeosci 122:1011–1021. https://doi.org/10.1002/2016JG003734

Iwata H, Nakazawa K, Sato H, Itoh M, Miyabara Y, Hirata R, Takahashi Y, Tokida T, Endo R (2020) Temporal and spatial variations in methane emissions from the littoral zone of a shallow mid-latitude lake with steady methane bubble emission areas. Agric Forest Meteorol 295:108184. https://doi.org/10.1016/j.agrformet.2020.108184

Jeppesen E, Jensen JP, Søndergaard M, Lauridsen T (1999) Trophic dynamics in turbid and clearwater lakes with special emphasis on the role of zooplankton for water clarity. Hydrobiologia 408:217–231. https://doi.org/10.1023/A:1017071600486

Kankaala P, Huotari J, Peltomaa E, Saloranta T, Ojala A (2006) Methanotrophic activity in relation to methane efflux and total heterotrophic bacterial production in a stratified, humic, boreal lake. Limnol Oceanogr 51:1195–1204. https://doi.org/10.4319/lo.2006.51.2.1195

Kankaala P, Taipale S, Nykänen H, Jones RI (2007) Oxidation, efflux, and isotopic fractionation of methane during autumnal turnover in a polyhumic, boreal lake. J Geophys Res Biogeosci 112:1–7. https://doi.org/10.1029/2006JG000336

Kirchman D, Mitchell R (1982) Contribution of particle-bound bacteria to total microheterotrophic activity in five ponds and two marshes. Appl Environ Microbiol 43:200–209. https://doi.org/10.1128/aem.43.1.200-209.1982

Klaus M, Vachon D (2020) Challenges of predicting gas transfer velocity from wind measurements over global lakes. Aquat Sci 82:1–17. https://doi.org/10.1007/s00027-020-00729-9

Koenker R (2005) Quantile regression. Cambridge University Press. https://doi.org/10.1017/CBO9780511754098

Kotsyurbenko OR, Friedrich MW, Simankova MV, Nozhevnikova AN, Golyshin PN, Timmis KN, Conrad R (2007) Shift from acetoclastic to H_2-dependent methanogenesis in a West Siberian peat bog at low pH values and isolation of an acidophilic

Methanobacterium strain. Appl Environ Microbiol 73(7):2344–2348. https://doi.org/10.1128/AEM.02413-06

Lan X, Thoning KW, Dlugokencky EJ (2024). Trends in globally-averaged CH_4, N_2O, and SF_6 determined from NOAA global monitoring laboratory measurements. Version 2024–10 https://doi.org/10.15138/P8XG-AA10

Lauerwald R, Allen GH, Deemer BR, Liu S, Maavara T, Raymond P, Alcott L, Bastviken D, Hastie A, Holgerson MA, Johnson MS, Lehner B, Lin P, Marzadri A, Ran L, Tian H, Yang X, Yao Y, Regnier P (2023) Inland water greenhouse gas budgets for RECCAP2: 2 regionalization and homogenization of estimates. Global Biogeochem Cycles 37:e2022GB007658. https://doi.org/10.1029/2022GB007658

Li C, Hambright KD, Bowen HG, Trammell MA, Grossart HP, Burford MA, Hamilton DP, Jiang H, Latour D, Meyer EI, Padisák J, Zamor RM, Krumholz LR (2021) Global co-occurrence of methanogenic archaea and methanotrophic bacteria in microcystis aggregates. Environ Microbiol. https://doi.org/10.1111/1462-2920.15691

Liptay K, Chanton J, Czepiel P, Mosher B (1998) Use of stable isotopes to determine methane oxidation in landfill cover soils. J Geophys Res Atmos 103(D7):8243–8250. https://doi.org/10.1029/97JD02630

Liu Y, Conrad R, Yao T, Gleixner G, Claus P (2017) Change of methane production pathway with sediment depth in a lake on the Tibetan plateau. Palaeogeogr Palaeoclimatol Palaeoecol 474:279–286. https://doi.org/10.1016/j.palaeo.2016.06.021

Lopes F, Viollier E, Thiam A, Michard G, Abril G, Groleau A, Prévot F, Carrias J-F, Albéric P, Jézéquel D (2011) Biogeochemical modelling of anaerobic vs. aerobic methane oxidation in a meromictic crater lake (Lake Pavin, France). Appl Geochem 26:1919–1932. https://doi.org/10.1016/j.apgeochem.2011.06.021

MacIntyre S, Jonsson A, Jansson M, Aberg J, Turney DE, Miller SD (2010) Buoyancy flux, turbulence, and the gas transfer coefficient in a stratified lake. Geophys Res Lett 37(24):L24604. https://doi.org/10.1029/2010gl044164

Malghani S, Reim A, von Fischer J, Conrad R, Kuebler K, Trumbore SE (2016) Soil methanotroph abundance and community composition are not influenced by substrate availability in laboratory incubations. Soil Biol Biochem 101:184–194. https://doi.org/10.1016/j.soilbio.2016.07.009

Mayr MJ, Zimmermann M, Dey J, Brand A, Wehrli B, Bürgmann H (2020) Growth and rapid succession of methanotrophs effectively limit methane release during lake overturn. Commun Biol 3:108. https://doi.org/10.1038/s42003-020-0838-z

McGinnis DF, Greinert J, Artemov Y, Beaubien SE, Wüest A (2006) The fate of rising methane bubbles in stratified waters: what fraction reaches the atmosphere? J Geophys Res 111:C09007. https://doi.org/10.1029/2005JC003183

Meier D, van Grinsven S, Michel A, Eickenbusch P, Glombitza C, Han X, Fiskal A, Bernasconi S, Schubert CJ, Lever MA (2024) Hydrogen–independent CO_2 reduction dominates methanogenesis in five temperate lakes that differ in trophic states. ISME Commun 4:ycae089. https://doi.org/10.1093/ismeco/ycae089

Morana C, Borges AV, Roland FAE, Darchambeau F, Descy J-P, Bouillon S (2015) Methanotrophy within the water column of a large meromictic tropical lake (Lake Kivu, East Africa). Biogeosciences 12:2077–2088. https://doi.org/10.5194/bg-12-2077-2015

Morana C, Bouillon S, Nolla-Ardèvol V, Roland FAE, Okello W, Descy J-P, Nankabirwa A, Nabafu E, Springael D, Borges AV (2020) Methane paradox in tropical lakes? Sedimentary fluxes rather than pelagic production in oxic conditions sustain methanotrophy and emissions to the atmosphere. Biogeosciences 17:5209–5221. https://doi.org/10.5194/bg-17-5209-2020

Murase J, Sugimoto A (2005) Inhibitory effect of light on methane oxidation in the pelagic water column of a mesotrophic lake (Lake Biwa, Japan). Limnol Oceanogr 50:1339–1343. https://doi.org/10.4319/lo.2005.50.4.1339

Ni R, Xu C, Shi X, Yang S, Li L, Peng X, Song L (2022) Acetoclastic methanogenesis pathway stability despite the high microbial taxonomic variability in the transition from acidogenesis to methanogenesis during food waste anaerobic digestion. J Clean Prod 372:133758. https://doi.org/10.1016/j.jclepro.2022.133758

Peretyatko A, Teissier S, De Backer S, Triest L (2012) Biomanipulation of hypereutrophic ponds: when it works and why it fails. Environ Monit Assess 184:1517–1531. https://doi.org/10.1007/s10661-011-2057-z

Peretyatko A, Symoens JJ, Triest L (2007). Impact of macrophytes on phytoplankton in eutrophic peri-urban ponds, implications for pond management and restoration. Belgian Journal of Botany, pp. 83–99. https://www.jstor.org/stable/20794626

R Core Team (2022). R: a language and environment for statistical computing. R Foundation for Statistical Computing, Vienna, Austriaa. https://www.R-project.org/.

Reis PCJ, Ruiz-González C, Soued C, Crevecoeur S, Prairie YT (2020) Rapid shifts in methanotrophic bacterial communities mitigate methane emissions from a tropical hydropower reservoir and its downstream river. Sci Total Environ 748:141374. https://doi.org/10.1016/j.scitotenv.2020.141374

Reis PCJ, Thottathil SD, Prairie YT (2022) The role of methanotrophy in the microbial carbon metabolism of temperate lakes. Nat Commun 13:43. https://doi.org/10.1038/s41467-021-27718-2

Roland FAE, Darchambeau F, Crowe S, Morana C, Borges AV (2018) Anaerobic methane oxidation in an East African great lake (Lake Kivu). J Great Lake Res. https://doi.org/10.1016/j.jglr.2018.04.003

Rosentreter JA, Borges AV, Deemer BR, Holgerson MA, Liu S, Song C, Melack J, Raymond PA, Duarte CM, Allen GH, Olefeldt D, Poulter B, Battin TI, Eyre BD (2021) Half of global methane emissions come from highly variable aquatic ecosystem sources. Nat Geosci 14:225–230. https://doi.org/10.1038/s41561-021-00715-2

Rudd JWM, Hamilton RD (1978) Methane cycling in a eutrophic shield lake and its effects on whole lake metabolism. 1. Limnol Oceanogr. https://doi.org/10.4319/lo.1978.23.2.0337

Rudd JWM, Hamilton RD, Campbell NER (1974) Measurement of microbial oxidation of methane in lake water. Limnol Oceanogr 19:519–524. https://doi.org/10.4319/lo.1974.19.3.0519

Scheffer M, van Nes EH (2007) Shallow lakes theory revisited: various alternative regimes driven by climate, nutrients, depth and lake size. Hydrobiologia 584:455–466. https://doi.org/10.1007/s10750-007-0616-7

Scheffer M, Hosper SH, Meijer ML, Moss B, Jeppesen E (1993) Alternative equilibria in shallow lakes. Trends Ecol Evol 8:275–279. https://doi.org/10.1016/0169-5347(93)90254-M

Schenk J, Sawakuchi HO, Sieczko AK, Pajala G, Rudberg D, Hagberg E, Fors K, Laudon H, Karlsson J, Bastviken D (2021) Methane in lakes: variability in stable carbon isotopic composition and the potential importance of groundwater input. Front Earth Sci. https://doi.org/10.3389/feart.2021.722215

Schulz S, Conrad R (1996) Influence of temperature on pathways to methane production in the permanently cold profundal sediment of Lake Constance. FEMS Microbiol Ecol. https://doi.org/10.1111/j.1574-6941.1996.tb00299.x

Schulz S, Matsuyama H, Conrad R (1997) Temperature dependence of methane production from different precursors in a profundal sediment (Lake Constance). FEMS Microbiol Ecol 22:207–213. https://doi.org/10.1111/j.1574-6941.1997.tb00372.x

Shelley F, Grey J, Trimmer M (2014) Widespread methanotrophic primary production in lowland chalk rivers. Proc R Soc Lond B Biol Sci 281:20132854. https://doi.org/10.1098/rspb.2013.2854

Singleton CM, McCalley CK, Woodcroft BJ, Boyd JA, Evans PN, Hodgkins SB, Chanton JP, Frolking S, Crill PM, Saleska SR, Rich VI, Tyson GW (2018) Methanotrophy across a natural permafrost thaw environment. ISME J 12:2544–2558. https://doi.org/10.1038/s41396-018-0065-5

Sturm A, Fowle DA, Jones C, Leslie K, Nomosatryo S, Henny C, Canfield DE, Crowe SA (2019) Rates and pathways of CH_4 oxidation in ferruginous Lake Matano, Indonesia. Geobiology 17:294–307. https://doi.org/10.1111/gbi.12325

Su G, Tolu J, Glombitza C, Zopfi J, Lehmann MF, Lever MA, Schubert CJ (2025) Methanogenesis by CO_2 reduction dominates lake sediments with different organic matter compositions. Biogeosciences 22:4449–4466. https://doi.org/10.5194/bg-22-4449-2025

Templeton AS, Chu K-H, Alvarez-Cohen L, Conrad ME (2006) Variable carbon isotope fractionation expressed by aerobic CH_4-oxidizing bacteria. Geochim Cosmochim Acta 70:1739–1752. https://doi.org/10.1016/j.gca.2005.12.002

Thottathil SD, Reis PCJ, del Giorgio PA, Prairie YT (2018) The extent and regulation of summer methane oxidation in northern lakes. J Geophys Res Biogeosci 123:3216–3230. https://doi.org/10.1029/2018JG004464

Thottathil SD, Reis PCJ, Prairie YT (2019) Methane oxidation kinetics in northern freshwater lakes. Biogeochemistry 143:105–116. https://doi.org/10.1007/s10533-019-00552-x

Utsumi M, Nojiri Y, Nakamura T, Nozawa T, Otsuki A, Seki H (1998) Oxidation of dissolved methane in a eutrophic, shallow lake: Lake Kasumigaura. Japan. Limnol Oceanogr 43:471e480. https://doi.org/10.4319/lo.1998.43.3.0471

Vachon D, Prairie YT (2013) The ecosystem size and shape dependence of gas transfer velocity versus wind speed relationships in lakes. Can J Fish Aquat Sci 70(12):1757–1764

Van Onsem S, De Backer S, Triest L (2010) Microhabitat–zooplankton relationship in extensive macrophyte vegetations of eutrophic clear-water ponds. Hydrobiologia 656:67–81. https://doi.org/10.1007/s10750-010-0442-1

Vicente I. de A, Amores V, Cruz-Pizarro L (2006) Instability of shallow lakes: a matter of the complexity of factors involved in sediment and water interaction? Limnetica 25(1–2):253–270. https://doi.org/10.23818/limn.25.18

Wang Z, Wang S, Hu Y, Du B, Meng J, Wu G, Liu H, Zhan X (2022) Distinguishing responses of acetoclastic and hydrogenotrophic methanogens to ammonia stress in mesophilic mixed cultures. Water Res 224:119029. https://doi.org/10.1016/j.watres.2022.119029

Wang T, Zhumabieke M, Zhang N, Liu C, Zhong J, Liao Q, Zhang L (2023) Variable promotion of algae and macrophyte organic matter on methanogenesis in anaerobic lake sediment. Environ Res 237:116922. https://doi.org/10.1016/j.envres.2023.116922

Wanninkhof R (1992) Relationship between wind speed and gas exchange over the ocean. J Geophys Res Oceans 97:7373–7382. https://doi.org/10.1029/92JC00188

Weiss RF (1981) Determinations of carbon dioxide and methane by dual catalyst flame ionization chromatography and nitrous oxide by electron capture chromatography. J Chromatogr Sci 19:611–616. https://doi.org/10.1093/chromsci/19.12.611

West WE, Coloso JJ, Jones SE (2012) Effects of algal and terrestrial carbon on methane production rates and methanogen community structure in a temperate lake sediment. Freshw Biol 57:949–955. https://doi.org/10.1111/j.1365-2427.2012.02755.x

Whiticar MJ (1999) Carbon and hydrogen isotope systematics of bacterial formation and oxidation of methane. Chem Geol 161:291–314. https://doi.org/10.1016/S0009-2541(99)00092-3

Whiticar MJ, Faber E, Schoell M (1986) Biogenic methane formation in marine and freshwater environments: CO_2 reduction vs. acetate fermentation—isotope evidence. Geochim Cosmochim Acta 50(5):693–709. https://doi.org/10.1016/0016-7037(86)90346-7

Winfrey MR, Zeikus JG (1979) Microbial methanogenesis and acetate metabolism in a meromictic lake. Appl Environ Microbiol 37:213–221. https://doi.org/10.1128/aem.37.2.213-221

Xu L, Zhuang GC, Montgomery A, Liang Q, Joye SB, Wang F (2021) Methyl-compounds driven benthic carbon cycling in the sulfate-reducing sediments of South China Sea. Environ Microbiol 23:641–651. https://doi.org/10.1111/1462-2920.15110

Yamamoto S, Alcauskas JB, Crozier TE (1976) Solubility of methane in distilled water and seawater. J Chem Eng Data 21:78–80. https://doi.org/10.1021/je60068a029

Yang Y, Chen J, Tong T, Xie S, Liu Y (2020) Influences of eutrophication on methanogenesis pathways and methanogenic microbial community structures in freshwater lakes. Environ Pollut 260:114106. https://doi.org/10.1016/j.envpol.2020.114106

Yentsch CS, Menzel DW (1963) A method for the determination of phytoplankton chlorophyll and phaeophytin by fluorescence. Deep Sea Res 10:221–231. https://doi.org/10.1016/0011-7471(63)90358-9

Zeikus JG, Winfrey MR (1976) Temperature limitation of methanogenesis in aquatic sediments. Appl Environ Microbiol 31:99–107. https://doi.org/10.1128/aem.31.1.99-107.1976